J. Am. Chem. Soc. **1989**, *111*, 8156–8160

These might possibly be due to an incomplete absorption correction; however, attempts at improving the correction did not improve the bonds. Looking at the ORTEP plots it is evident that the groups at P(36) definitely have much larger thermal vibrations. The weakly bonded W–O distances are W(1)–O(20) = 2.635 (17) Å and W(2)–O(35) = 2.708 (14) Å. The closest intramolecular contact for the two non-bonded O's are O(20)–O(3) = 2.92 Å and O(35)–O(11) = 2.99 Å. The closest intermolecular contacts are O(20) to C(24) = 4.21 Å and O(35) to C(8) = 3.29 Å. The final difference map still had several peaks of ~2.5 e/Å^3 in the close vicinity of the W atoms. The molecule has an approximate 2-fold axis perpendicular to the W(1)–W(2) bond.

Acknowledgment. We thank the National Science Foundation for support. W.E.B. acknowledges a Chester Davis Fellowship for 1986–1987.

Supplementary Material Available: Tables of anisotropic thermal parameters, bond distances, and bond angles for $Mo_2(O_2CP(t\text{-}Bu)_2)_4 \cdot 2C_6H_6$ and $W_2(NMe_2)_2(O_2CNMe_2)_2(O_2CP(t\text{-}Bu)_2)_2$ (11 pages); observed and calculated structure factors (19 pages). Ordering information is given on any current masthead page.

Ligand Dependence of Electronic Configuration of the Rh–Rh Bond in Rh_2^{5+} Complexes As Studied by Electron Spin Resonance and Electrochemistry

Takashi Kawamura,*[1a] Hiroaki Katayama,[1b] Hiroyuki Nishikawa,[1c] and Tokio Yamabe[1b,c]

Contribution from the Department of Chemistry, Faculty of Engineering, Gifu University, Yanagido, Gifu 501-11, Japan, and the Division of Molecular Engineering and the Department of Hydrocarbon Chemistry, Faculty of Engineering, Kyoto University, Kyoto 606, Japan.
Received February 20, 1989

Abstract: Electron spin resonance spectra of Rh_2^{5+} radicals derived from $Rh_2(O_2CCH_3)_4L_2$, where L is H_2O, CH_3OH, *i*-PrOH, THF, $(CH_3)_2CO$, CH_3CN, and Cl^-, show abnormally large shifts of the principal values of their **g** tensors from the free-spin value ($g_e = 2.0023$): $g_\parallel = 3.38–4.00$ and $g_\perp = 0.6–1.87$. These large shifts indicate that the orbital angular momentum of the odd electron in these radicals is not quenched; namely the odd-electron orbital is degenerate. The assignment of $\sigma^2\pi^4\delta^2\delta^{*2}\pi^{*3}$ to the electronic configuration of their Rh–Rh bonds is the most reasonable one satisfying these observations. Cationic radicals generated from $Rh_2(O_2CCH_3)_{4-n}[CH_3C(O)NH]_n(CH_3CN)_2$, where $n = 1–4$, have been reported to have $g_\parallel < g_e$ and $g_\perp > g_e$. This is consistent with the electronic configuration of $\sigma^2\pi^4\delta^2\pi^{*4}\delta^{*1}$ for their Rh–Rh bonds. Those Rh_2^{4+} complexes, of which Rh_2^{5+} radicals have an odd electron accommodated in the $\pi_{RhRh}{}^*$ orbital, have high oxidation potentials (0.58–0.77 V vs Fc^+/Fc, where Fc designates ferrocene). Those Rh_2^{4+} complexes, of which Rh_2^{5+} radicals have an odd electron in the $\delta_{RhRh}{}^*$ orbital, show low oxidation potentials (–0.33 to +0.49 V vs Fc^+/Fc). The latter complexes have amidate or amidinate bridging ligands. These observations show that a substitution of amidate or amidinate ligands for bridging carboxylates results in an enhanced destabilization of the $\delta_{RhRh}{}^*$ orbital. This destabilization should be induced by an increased mixing of ligand π orbitals into the $\delta_{RhRh}{}^*$ orbital in a π-antibonding phase between the Rh atom and the bridging ligand. An appreciable delocalization of the σ_{RhRh} orbital onto bridging ligands is also proposed in connection with a dependence of oxidation potentials on bridging ligands.

Over the past two decades a substantial number of reports have appeared describing preparations and accurate geometries of Rh_2^{4+} complexes.[2-7] Spectroscopic characterizations of this class of complexes lend insight into electronic structures of metal–metal bonds. Electron spin resonance (ESR) studies of Rh_2^{5+} complexes have shown an unexpected dependence of the electronic configuration of the Rh–Rh bond on the ligands. Complexes with axial ligands of phosphines and phosphites[8,9] have been shown to have the electronic configuration of $\pi^4\delta^2\delta^{*2}\pi^{*4}\sigma^1$.[8] This has been reproduced by molecular orbital calculations.[10,11]

The configuration of the Rh–Rh bond in $[Rh_2(O_2CCH_3)_4(H_2O)_2]^{\bullet+}$ has been calculated to be $\sigma^2\pi^4\delta^2\pi^{*4}\delta^{*1}$ by an SCF–Xα–SW method[12] and to be $\pi^4\delta^2\delta^{*2}\pi^{*4}\sigma^1$ by an ab initio unrestricted Hartree–Fock method,[11] respectively. In contrast to both of the predictions, our preliminary ESR study has shown that this aquo complex has the configuration of $\sigma^2\pi^4\delta^2\delta^{*2}\pi^{*3}$.[13] Subsequently this experimental result has been reproduced by calculations with an ab initio Hartree–Fock CI method.[14] The CI expansion has been necessary to describe *localization* of positive

---

[1] (a) Gifu University. (b) The Division of Molecular Engineering, Kyoto University. (c) The Department of Hydrocarbon Chemistry, Kyoto University.

[2] Cotton, F. A.; Walton, R. A. *Multiple Bonds Between Metal Atoms*; Wiley-Interscience: New York, 1982.

[3] Felthouse, T. R. *Prog. Inorg. Chem.* **1982**, *29*, 73.

[4] Boyer, E. B.; Robinson, S. D. *Coord. Chem. Rev.* **1983**, *50*, 109.

[5] Lifsey, R. S.; Lin, X. Q.; Chavan, M. Y.; Ahsan, M. Q.; Kadish, K. M.; Bear, J. L. *Inorg. Chem.* **1987**, *26*, 830, and references cited therein.

[6] Piraino, P.; Bruno, G.; Tresoldi, G.; Lo Schiavo, S.; Zanello, P. *Inorg. Chem.* **1987**, *26*, 91.

[7] Dunbar, K. R. *J. Am. Chem. Soc.* **1988**, *110*, 8247.

[8] (a) Kawamura, T.; Fukamachi, K.; Hayashida, S. *J. Chem. Soc., Chem. Commun.* **1979**, 945. (b) Kawamura, T.; Fukamachi, K.; Sowa, T.; Hayashida, S.; Yonezawa, T. *J. Am. Chem. Soc.* **1981**, *103*, 364.

[9] Chavan, M. Y.; Zhu, T. Pp.; Lin, X. Q.; Ahsan, M. Q.; Bear, J. L.; Kadish, K. M. *Inorg. Chem.* **1984**, *23*, 4538.

[10] Burnsten, B. E.; Cotton, F. A. *Inorg. Chem.* **1981**, *20*, 3042.

[11] Nakatsuji, H.; Onishi, Y.; Ushio, J.; Yonezawa, T. *Inorg. Chem.* **1983**, *22*, 1623.

[12] Norman, J. D., Jr.; Renzoni, G. E.; Case, D. A. *J. Am. Chem. Soc.* **1979**, *101*, 5256.

[13] Kawamura, T.; Katayama, H.; Yamabe, T. *Chem. Phys. Lett.* **1986**, *130*, 20.

[14] Mougenot, P.; Demuynck, J.; Bênard, M. *Chem. Phys. Lett.* **1987**, *136*, 279.

0002-7863/89/1511-8156$01.50/0

Table I. Electronic Absorption Spectra of $[Rh_2(O_2CCH_3)_4L_2]^{\bullet+}$

ligand	solvent	λ/nm (log ε)
Cl^-	0.02 M LiCl, 1 M $HClO_4$(aq)	782 (2.426), 523 (2.404), 415 (2.740), 320 (3.086) (sh), 260 (3.705) (sh), 240 (3.969) (sh), 220 (4.133) (sh)
CH_3CN	CH_3CN	1070 (1.619) (sh), 791 (2.396), 388 (2.645) (sh), 330 (2.984) (sh), 263 (3.770), 240 (3.782) (sh)
H_2O	1 M $HClO_4$(aq)	755 (2.396), 514 (2.385), 365 (2.517) (sh), 320 (1.664) (sh), 235 (3.979) (sh), 210 (4.110) (sh)
MeOH	MeOH	772 (2.271), 518 (2.204), 324 (3.054) (sh), 244 (3.951) (sh), 212 (4.079) (sh)

holes of π^* and δ^* symmetry.[14] We have also proposed an assignment of the $\sigma^2\pi^4\delta^2\pi^{*4}\delta^{*1}$ configuration to $\{Rh_2[CH_3C(O)NH]_n(O_2CCH_3)_{4-n}(CH_3CN)_2\}^{\bullet+}$ for n = 1–4.[13]

Only $[Rh_2(O_2CCH_3)_4(H_2O)_2]^{\bullet+}$ has been reported to have the $\pi_{RhRh}{}^*$ odd-electron orbital. In this paper we will show that the odd electron is accommodated in the $\pi_{RhRh}{}^*$ orbital in Rh_2^{5+} radicals derived from dirhodium tetraacetate with axial ligands of tetrahydrofuran (THF), alcohols, acetone, acetonitrile, and chloride ion.

We will search for dominant electronic interactions that induce the ligand-dependent change of the electronic configuration by comparing oxidation potentials of Rh_2^{4+} complexes with symmetries of odd-electron orbitals of the corresponding Rh_2^{5+} radicals. This comparison will reveal that the substitution of an amidate or an amidinate for a bridging carboxylate induces an enhanced destabilization of the $\delta_{RhRh}{}^*$ orbital. The delocalization of the σ_{RhRh} orbital onto the bridging ligands will be proposed as an origin of the bridging-ligand dependence of oxidation potentials of Rh_2^{4+} complexes with axial ligands of phosphines.

Experimental Section

Materials. $Rh_2(O_2CCH_3)_4(H_2O)_2$, $Rh_2(O_2CCH_3)_4$, and $Rh_2(O_2CCH_3)_4(H_2O)_2(ClO_4)$ were prepared by literature methods.[15,16] All organic solvents except THF were fractionally distilled and stored over molecular sieves 3A, which were vacuum oven dried. THF was fractionally distilled from benzophenone ketyl before use for electrochemical studies or vacuum transferred from sodium–potassium alloy for samples of measurements of ESR and electronic absorption spectra.

ESR and Electronic Absorption Spectra. Electronic spectra were observed on a Shimadzu UV-365 spectrophotometer at room temperature. ESR spectra were obtained on a JEOL PE-2X spectrometer modified with a JEOL ES-SCXA gunn diode microwave unit at a temperature between 4 and 20 K by using an Air Products LTR liquid-helium variable-temperature equipment or a liquid-helium cryostat. ESR microwave frequency was counted on a Takedariken TR-5501 frequency counter equipped with a TR-5023 frequency converter. Field sweep was monitored by using an Echo Electronics EFM-2000 proton NMR field meter.

Samples of organic solutions for measurement of electronic absorption spectra were prepared by utilizing a reaction flask that was connected to a vacuum line. A quartz UV–vis cell (1-cm path length) has been fused to the reaction flask. A purified and dried solvent was transferred in a vacuum line onto $Rh_2(O_2CCH_3)_4(H_2O)_2(ClO_4)$ in the reaction flask to dissolve the radical salt, and then the solvent was evaporated to complete dryness. After several distillation–dissolution–evaporation cycles for the thorough exchange of the axial ligands from the original H_2O to the solvent molecule, the solution was frozen and the flask was sealed off and submitted to measurements.

For the measurement of electronic absorption spectra of aqueous solutions of $[Rh_2O_2CCH_3)_4(H_2O)_2]^{\bullet+}$ or $[Rh_2(O_2CCH_3)_4(Cl)_2]^{\bullet-}$, $Rh_2(O_2CCH_3)_4(H_2O)_2(ClO_4)$ was dissolved under argon atmosphere into pure H_2O and 1 mol/L $HClO_4$ aqueous solution or 1 mol/L $HClO_4$ aqueous solution containing 0.02 mol/L LiCl,[17] respectively.

Samples for ESR measurements were prepared in a manner similar to those for electronic absorption spectra. The ESR sample of $[Rh_2(O_2CCH_3)_4(Cl)_2]^{\bullet-}$ was prepared by dissolving $Rh_2(O_2CCH_3)_4(H_2O)_2(ClO_4)$ in 1 mol/L $HClO_4$ aqueous solution containing 0.2 mol/L NaCl. Every solution of ESR measurement contained a paramagnetic complex in a concentration of ca. 10 mmol/L.

Electrochemistry. Cyclic voltammetry studies were conducted by using a Hokuto-Denko HB-107A function generator and HB-104A potentiostat/galvanostat and recorded on a Hitachi 057-1001 X-Y recorder. Both working and auxiliary electrodes were platinum wires. The reference electrode was a saturated calomel electrode (SCE), which was separated from the bulk of the solution by a sintered glass disk to prevent aqueous contaminations from entering the cell via the SCE.

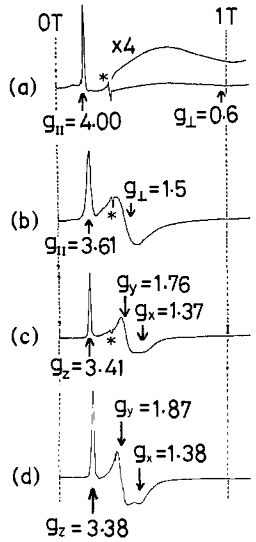

Figure 1. X-Band ESR spectra of $[Rh_2(O_2CCH_3)_4L_2]^{\bullet+}$: (a) L = Cl^- at 6 K; (b) L = H_2O at 4.2 K; (c) L = *i*-PrOH at 4.2 K; (d) L = THF at 4.2 K. Sharp signals with an asterisk are due to unidentified species.

The supporting electrolyte was tetra-*n*-butylammonium perchlorate (0.1 mol/L) for acetonitrile, acetone, and THF and sodium perchlorate (0.1 mol/L) for pure H_2O and methanol, respectively. To aqueous $HClO_4$ solutions extraneous supporting electrolyte was not added. To these electrolyte solutions was added axial ligand-free $Rh_2(O_2CCH_3)_4$, and the resultant solutions were submitted to cyclic voltammetry studies. The solution of $[Rh_2(O_2CCH_3)_4(Cl)_2]^{2-}$[18] was prepared by dissolving $Rh_2(O_2CCH_3)_4(H_2O)_2$ in 2.7 mol/L NaCl aqueous solution containing 1 mol/L $HClO_4$. Electrolyte solutions contained ca. 1 mmol/L of a dirhodium complex.

After observation of a cyclic voltammogram of a complex in a nonaqueous solutions, that of ferrocene (1 mmol/L) was recorded in a similar electrolyte solution by using the same reference SCE. The cyclic voltammograms of ferrocene were used to correct for variable potential differences of liquid junctions.

Results

Electronic and ESR Spectra. Cationic radicals, $[Rh_2(O_2CCH_3)_4L_2]^{\bullet+}$ [L = CH_3CN, $(CH_3)_2CO$, CH_3OH, *i*-PrOH, and THF], were prepared by repeated cycles of dissolution of $Rh_2(O_2CCH_3)_4(H_2O)_2(ClO_4)$[16] in vacuum-transferred dry organic solvent followed by evaporation to complete dryness to replace the original H_2O axial ligand with the organic solvent molecule. The replacement was monitored by electronic absorption spectra. In the case of the preparation of $[Rh_2(O_2CCH_3)_4(CH_3CN)_2]^{\bullet+}$, for example, the substitution was confirmed by the coincidence of its absorption spectrum in the region of 450–900 nm with that reported by Kadish and his co-workers.[9] Dissolution of $Rh_2(O_2CCH_3)_4(H_2O)_2(ClO_4)$ in a NaCl aqueous solution acidified with $HClO_4$ generates $[Rh_2(O_2CCH_3)_4(Cl)_2]^{\bullet-}$ as has been pointed out by Cannon and his co-worker.[17] We have unsuccessfully tried to generate $[Rh_2(O_2CCH_3)_4(Br)_2]^{\bullet-}$ by dissolving $Rh_2(O_2CCH_3)_4(H_2O)_2(ClO_4)$ in an aqueous KBr solution and that of $\{Rh_2(O_2CCH_3)_4[N(CH_3)_3]_2\}^{\bullet+}$ by addition of the Rh_2^{5+} aquo

---

[15] Rempel, G. A.; Legzdins, P.; Smith, H.; Wilkinson, G.; Ucko, D. A. *Inorg. Synth.* **1972**, *13*, 90.

[16] (a) Moszner, M.; Ziolkowski, J. J. *Bull. Acad. Pol. Sci., Ser. Sci. Chim.* **1976**, *24*, 433. (b) Ziolkowski, J. J.; Moszner, M.; Glowiak, T. *J. Chem. Soc., Chem. Commun.* **1977**, 760.

[17] Cannon, R. D.; Powell, D. B.; Sarawek, K.; Stillman (nee Lund), J. S. *J. Chem. Soc., Chem. Commun.* **1976**, 31.

[18] Miskowski, V. M.; Scheafer, W. P.; Sadeghi, B.; Santarsiero, B. D.; Gray, H. B. *Inorg. Chem.* **1984**, *23*, 1154.

Table II. Principal Values of g Tensors of $Rh_2^{\bullet 5+}$ Radicals

radical	$g_{\parallel}$ (g_{zz})	$g_{\perp}$
$[Rh_2(O_2CCH_3)_4(Cl)_2]^{\bullet -}$/0.2 M NaCl + 1 M $HClO_4$(aq)	4.00	0.6
$[Rh_2(O_2CCH_3)_4(CH_3CN)_2]^{\bullet +}$/$CH_3CN$	3.90	0.6
$[Rh_2(O_2CCH_3)_4(H_2O)_2]^{\bullet +}$/1 M HClO(aq)	3.76	1.2
$[Rh_2(O_2CCH_3)_4(Me_2CO)_2]^{\bullet +}$/$Me_2CO$	3.69	1.04
$[Rh_2(O_2CCH_3)_4(H_2O)_2]^{\bullet +}$/$H_2O$	3.61	1.5
$[Rh_2(O_2CCH_3)_4(MeOH)_2]^{\bullet +}$/MeOH	3.61	1.33[a] 1.64[b]
$[Rh_2(O_2CCH_3)_4(i\text{-}PrOH)_2]^{\bullet +}$/*i*-PrOH	3.41	1.37[a] 1.76[b]
$[Rh_2(O_2CCH_3)_4(THF)_2]^{\bullet +}$/THF	3.38	1.38[a] 1.87[b]

[a] g_{xx}. [b] g_{yy}.

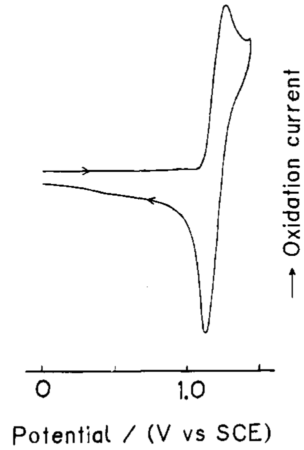

Figure 2. Cyclic voltammogram (V vs SCE) of $Rh_2(O_2CCH_3)_4$ at a platinum electrode in acetone containing 0.1 mol/L n-Bu_4NClO_4 at a scan rate of 0.1 V s^{-1}.

complex in trimethylamine. The Rh_2^{5+} complexes decomposed in these trials.

Table I summarizes electronic spectroscopy data of Rh_2^{5+} complexes. Figure 1 illustrates some of ESR spectra of the Rh_2^{5+} radicals observed at temperatures below 10 K. Very low temperatures were necessary to observe these spectra. ESR spectra of $[Rh_2(O_2CCH_3)_4(Cl)_2]^{\bullet -}$ and $[Rh_2(O_2CCH_3)_4L_2]^{\bullet +}$ [L = CH_3CN, H_2O, and $(CH_3)_2CO$] were broad and axially symmetric, whereas those of $[Rh_2(O_2CCH_3)_4L_2]^{\bullet +}$ (L = CH_3OH, *i*-PrOH, and THF) were rhombic. The principal values of their g tensors are listed in Table II.

Cyclic Voltammetry. Figure 2 shows the cyclic voltammetric response at a platinum electrode given by $Rh_2(O_2CCH_3)_4$ in dry acetone containing 0.1 mol/L n-Bu_4NClO_4 as supporting electrolyte. The half-wave oxidation potential, $E_{1/2}$, and the peak separation were 1.17 V vs. SCE and 90 mV, respectively. Ligand-free dirhodium tetraacetate dissolved in dry acetonitrile, methanol, and THF showed similar cyclic voltammetric responses.

Each measurement was followed by that of ferrocene in a same electrolyte solution. The oxidation potential of ferrocene in each solvent was used to obtain that of the Rh_2^{4+} complex relative to the ferrocenium ion/ferrocene potential in order to correct for variable liquid-junction potentials. For the conversion of the potentials in the aqueous solutions, the oxidation potential of ferrocene in aqueous solutions is assumed to be 0.150 V vs SCE.[19] Table III reports half-wave oxidation potentials of Rh_2^{4+} complexes.

Discussion

ESR. The principal values of the g tensors in Table II are abnormally shifted from the free-electron value (g_e = 2.0023). The ESR spectra in Figure 1 are exceptionally broad, and we could observe them only at very low temperatures (<20 K). All these features indicate that the orbital angular momentum of the odd electron is reserved in $[Rh_2(O_2CCH_3)_4(Cl)_2]^{\bullet -}$ and $[Rh_2(O_2CCH_3)_4L_2]^{\bullet +}$, where L is CH_3CN, H_2O, $(CH_3)_2CO$, CH_3OH, *i*-PrOH, and THF. The reservation is equivalent to the fact that the odd-electron orbital is degenerate or nearly degenerate. This type of abnormal ESR spectra has been reported for hemoglobin azide[20] and ferrocenium cation,[21] which have degenerate odd-electron orbitals.

Table III. Oxidation Potentials (V vs Fc^+/Fc) for the Anodic Oxidation of $Rh_2(O_2CCH_3)_4L_2$

compound/solvent	$E_{1/2}$/V (vs Fc^+/Fc)
$Rh_2(O_2CCH_3)_4(MeOH)_2$/MeOH	0.58
$Rh_2(O_2CCH_3)_4(THF)_2$/THF	0.62
$[Rh_2(O_2CCH_3)_4(Cl)_2]^{2-}$/2.7 M NaCl + 1 M $HClO_4$(aq)	0.67
$Rh_2(O_2CCH_3)_4(Me_2CO)_2$/$Me_2CO$	0.67
$Rh_2(O_2CCH_3)_4(H_2O)_2$/H_2O	0.74
$Rh_2(O_2CCH_3)_4(H_2O)_2$/1 M $HClO_4$(aq)	0.75
$Rh_2(O_2CCH_3)_4(CH_3CN)_2$/$CH_3CN$	0.77

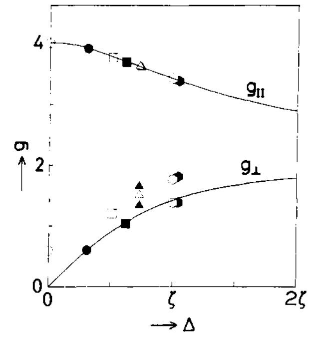

Figure 3. Dependence of the g tensor of Rh_2^{5+} radicals on the energy difference Δ given by eq 1 and 2 (solid lines) and plots of experimental values. $[Rh_2(OAc)_4(L)]^{\bullet -}$: ○, L = Cl in acidic NaCl aqueous solution. $[Rh_2(OAc)_4(L)_2]^{\bullet +}$: ●, L = MeCN in MeCN; □, L = H_2O in acidic aqueous solution; ■, L = Me_2CO in Me_2CO; △, L = H_2O in pure water; ▲, L = MeOH in MeOH; ○, L = *i*-PrOH in *i*-PrOH; ●, L = THF in THF. The notation ζ designates the *l*–*s* coupling constant of the Rh 4d atomic orbital (968 cm^{-1}).

The degeneracy in the present complexes cannot be an accidental one, since several complexes have shown the same type of ESR spectra. The spin–orbit coupling Hamiltonian around the rhodium atoms should give rise to nonzero matrix elements between the degenerate odd-electron orbitals. The allowed choices for such odd-electron orbitals are bonding π_{RhRh} and antibonding π_{RhRh}^* orbitals, and the parallel axis of the spin Hamiltonian is the direction of the Rh–Rh bond for both of the choices. We choose the latter orbital, assigning the electronic configuration of $\sigma^2\pi^4\delta^2\delta^{*2}\pi^{*3}$ to the Rh–Rh bond.

In Table II, the decrease of $g_{\parallel}$ (g_{zz} in the case of the rhombic spectra) toward g_e is attended by the increase of $g_{\perp}$ (the average value of g_{xx} and g_{yy} in the case of the rhombic spectra) also toward g_e. The simultaneous shifts of the principal values toward g_e indicate the increased lifting of the degeneracy of the π_{RhRh}^* orbitals accompanied by partial quenching of the orbital angular momentum of the odd electron. In complexes with the axial ligands of alcohols and THF, the lift is comparable to the spin–orbit coupling constant of the Rh 4d atomic orbital (968 cm^{-1}),[22] and the molecular x and y directions are discriminated in their ESR spectra.

Analysis of ESR. The (almost) degenerate pair of ground configurations for the present Rh_2^{5+} complexes are $\pi_y^{*2}\pi_x^{*1}$ and $\pi_x^{*2}\pi_y^{*1}$, where π_x^* and π_y^* are the degenerate pair of π_{RhRh}^* molecular orbitals. A notation of Δ will designate the energy

---

[19] Bauer, D.; Breant, M. In *Electroanalytical Chemistry*; Bard, A. D., Ed.; Marcel Decker: New York, 1975; Vol. 8, p 306.

[20] Griffith, J. S. *Nature* **1957**, *180*, 30.

[21] Maki, A. H.; Berry, T. E. *J. Am. Chem. Soc.* **1965**, *87*, 4437.

[22] Dunn, T. M. *Trans. Faraday Soc.* **1961**, *57*, 1441.

difference between these two configurations. All other states are assumed to have very high energies and will be neglected for the moment. This simple model gives the following principal values for the **g** tensor[13]

$$g_\parallel = 2 + 2k^2 \sin 2\theta \tag{1}$$

$$g_\perp = 2|\cos 2\theta| \tag{2}$$

where k^2 denotes the weight of the Rh 4d atomic orbitals in each of the $\pi_{RhRh}{}^*$ molecular orbitals and is less than unity and θ is a function of the energy difference Δ defined as $\theta = \tan^{-1}[\gamma + (1 + \gamma^2)^{1/2}]$ and $\gamma = \Delta/(k^2\zeta)$, where ζ is the spin–orbit coupling constant of the Rh 4d atomic orbital.

Figure 3 illustrates the dependence of the **g** tensor on the energy difference Δ given by eq 1 and 2 together with experimental plots. The point on the abscissa for each of the plots was determined so as to fit the experimental $g_\parallel$ value in the theoretical curve. The general trend of the resulted plots of experimental $g_\perp$ values coincides satisfactorily with the theoretical curve. This confirms the assignment of the $\sigma^2\pi^4\delta^2\delta^{*2}\pi^{*3}$ configuration to the Rh–Rh bond in the present Rh_2^{5+} complexes.

The deviation of the theoretical curve from the experimental plots is due to the neglect of the contributions from the excited states in the theory. These contributions may be taken into account by a standard second-order perturbation treatment of both spin–orbit interactions and Zeeman effects of orbital angular momenta of electrons.[23,24] This gives no additional term to $g_\parallel$, and this principal value given by eq 1 is correct to the second order with respect to orbital angular momenta of electrons. The observed values of $g_\parallel$ for $[Rh_2(O_2CCH_3)_4(Cl)_2]^{\bullet-}$ and $[Rh_2(O_2CCH_3)_4(CH_3CN)_2]^{\bullet+}$ are 4.00 and 3.90, respectively. Note that 4.0 is the possible maximum value of $g_\parallel$ given by eq 1. These experimental values together with eq 1 reveal that the energy difference Δ is negligibly small in comparison to the spin–orbit coupling constant ζ in these two complexes and that the $\pi_{RhRh}{}^*$ orbital is not delocalized on the bridging ligands (i.e., $k^2 \sim 1$). The latter conclusion supports the results of molecular orbital calculations.[10–12,25,26]

The second-order terms shift and split $g_\perp$ into g_{xx} and g_{yy} by mixing of a_{1g}, b_{1g}, and b_{2g} (in the idealized D_{4h} geometry) molecular orbitals into the $\pi_{RhRh}{}^*$ orbitals through the spin-orbit coupling interactions. Important contributions to g_{xx} and g_{yy} would arise from $\delta_{RhRh} \rightarrow \pi_{RhRh}{}^*$, $\sigma_{RhRh} \rightarrow \pi_{RhRh}{}^*$, and $\pi_{RhRh} \rightarrow \sigma_{RhO}{}^*$ (b_{1g}) states, which are low-lying d–d excited states. Without knowledge of exact molecular orbitals, further meaningful analyses of the **g** tensors are too difficult.

Rh_2^{5+} Complexes with $\delta_{RhRh}{}^*$ Odd-Electron Orbitals. As has been pointed out sometime ago,[8b] Rh_2^{5+} complexes with their odd electrons accommodated in $\delta_{RhRh}{}^*$ orbitals are predicted to have **g** tensors with $g_\parallel < g_e$ and $g_\perp > g_e$. This is true for such Rh_2^{5+} complexes in which the spin–orbit coupling interactions are sufficiently small to be treated with a second-order perturbation method (then $|g - g_e|$ would be less than ca. 0.2) and the interactions involving the odd electron take place predominantly on the rhodium atoms. Since the following Rh_2^{5+} complexes have been reported to have such types of **g** tensors, we assign their odd-electron orbitals to $\delta_{RhRh}{}^*$: $[Rh_2(N_2Ph_2CPh)_4]^{\bullet+}$,[27] $\{Rh_2[HNC(O)CH_3]_{4-n}(O_2CCH_3)_n(CH_3CN)_2\}^{\bullet+}$ (n = 0–3),[9] and $\{Rh_2[HNC(O)CH_3]_{4-n}(O_2CCH_3)_n(Me_2SO)_2\}^{\bullet+}$ (n = 0–2).[9]

The present conclusion on the bridging ligand dependent interchange of the highest occupied level between $\pi_{RhRh}{}^*$ and $\delta_{RhRh}{}^*$ orbitals supports ab initio SCF CI calculations on $[Rh_2(O_2CH)_4(H_2O)_2]^{\bullet+}$.[14] These calculations have given a result that the $\delta_{RhRh}{}^*$ ionization potential is 0.2–0.3 eV *greater* than that of the $\pi_{RhRh}{}^*$ electron for $Rh_2(O_2CH)_4(H_2O)_2$. Our conclusion is also consistent with UV photoelectron studies reported for $Rh_2(mhp)_4$,[28] where mhp is 6-methyl-2-oxopyridinate, and for Rh_2^{4+} formamidinate complexes.[26] These photoelectron studies have shown that their $\delta_{RhRh}{}^*$ ionization potentials are 0.7–1.1 eV *smaller* than those of $\pi_{RhRh}{}^*$ electrons.

Scheme I

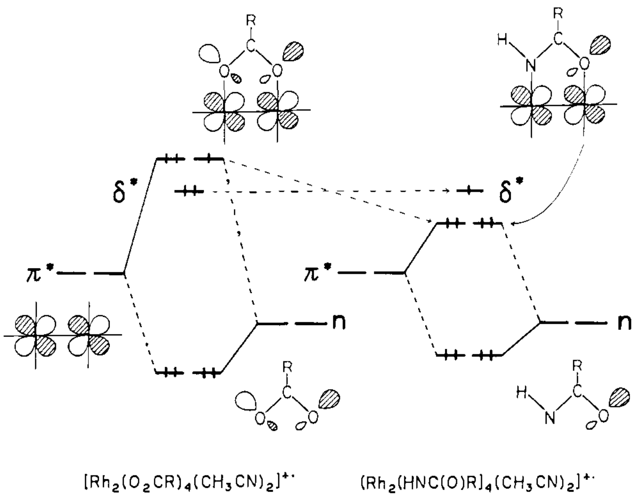

Scheme II

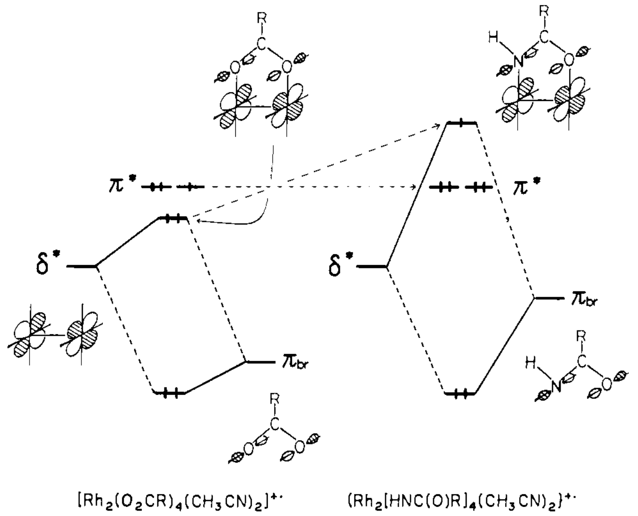

Cyclic Voltammetry. Since the first oxidation couple in cyclic voltammograms of the present $Rh_2(O_2CCH_3)_4$ complexes showed a peak-current ratio of 1.0 ± 0.1, and since present ESR studies have shown that the corresponding Rh_2^{5+} species are stable, we can assign this couple to a chemically reversible one-electron process. This is consistent with a number of studies on electrochemical behavior of Rh_2^{4+} complexes.[8b,9,27,29]

Interaction between Rh–Rh Bond and Ligand. Three types of electronic configurations of the Rh–Rh bond are now known for Rh_2^{5+} complexes. The configuration depends on both bridging and axial ligands. The electronic configurations and corresponding complexes are $\pi^4\delta^2\pi^{*4}\delta^{*2}\sigma^1$ for $[Rh_2(O_2CC_2H_5)_4(PPh_3)_2]^{\bullet+}$[8] and $\{Rh_2[NHC(O)CH_3]_4(PPh_3)_2\}^{\bullet+}$,[9] $\sigma^2\pi^4\delta^2\delta^{*2}\pi^{*3}$ for $[Rh_2(O_2CCH_3)_4(CH_3CN)_2]^{\bullet+}$, and $\sigma^2\pi^4\delta^2\pi^{*4}\delta^{*1}$ for $\{Rh_2[NHC(O)CH_3]_4(CH_3CN)_2\}^{\bullet+}$.

The strong σ donation from the phosphine to the Rh_2^{5+} core in $[Rh_2(O_2CC_2H_5)_4(PPh_3)_2]^{\bullet+}$ has given enhanced Rh–P σ-antibonding character to the σ_{RhRh} orbital. This character shifts the orbital to the highest occupied level.[8,10,30]

---

(23) Atherton, N. M. *Electron Spin Resonance, Theory and Applications*; Wiley: New York, 1973.

(24) Stone, A. J. *Proc. R. Soc. London* **1963**, *A271*, 424.

(25) (a) Norman, J. D., Jr.; Kolari, H. J. *J. Am. Chem. Soc.* **1978**, *100*, 791.

(26) Rizzi, G. A.; Casarin, M.; Tondello, E.; Piranio, P.; Granozzi, G. *Inorg. Chem.* **1987**, *26*, 3406.

(27) Le, J. C.; Chavan, M. Y.; Chau, L. K.; Bear, J. L.; Kadish, K. M. *J. Am. Chem. Soc.* **1985**, *107*, 7195.

(28) Berry, M.; Garner, C. D.; Hillier, I. H.; MacDowell, A. A. *J. Chem. Soc., Chem. Commun.* **1980**, 494.

(29) Piraino, P.; Schiavo, S. L.; Laschi, F.; Zanello, P. *Inorg. Chem.* **1987**, *26*, 2205.

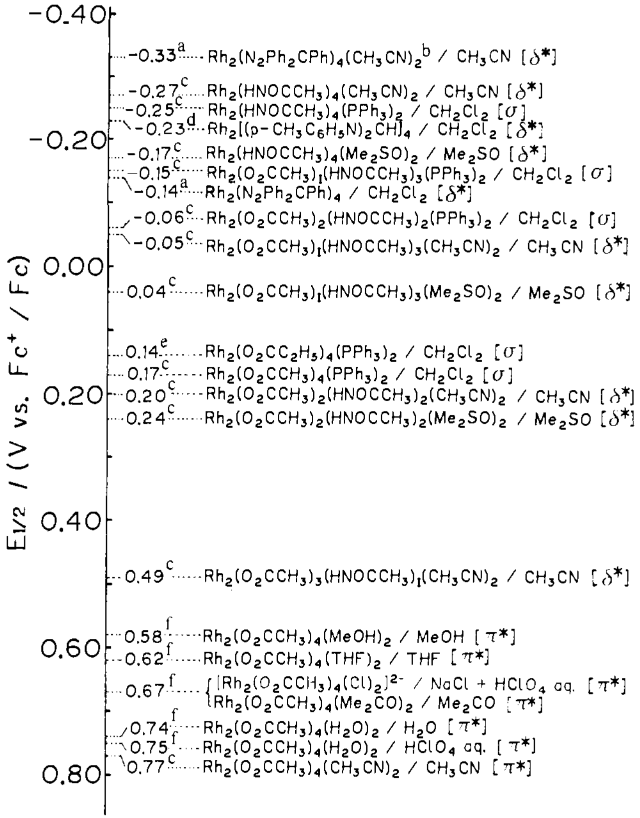

Figure 4. First oxidation potentials of Rh_2^{4+} complexes and symmetries of odd-electron orbitals of the corresponding Rh_2^{5+} radicals. Format: oxidation potential···Rh_2^{4+} complex/solvent [symmetry of odd-electron orbital]. Key: (a) ref 27; (b) number of the axial ligands remains uncertain; (c) ref 9; (d) ref 8b; (e) ref 29; (f) present work.

When the axial ligand is acetonitrile, the substitution of the bridging carboxylate ligands with acetamidate has induced an interchange of energy levels of $\delta_{RhRh}{}^*$ and $\pi_{RhRh}{}^*$ orbitals. Two models for the interchange are conceivable for electronic interactions between the Rh–Rh bond and the bridging ligands.

Scheme I shows interactions in the first model. The in-plane lone pair, n, on the oxygen atom shifts the energy level of the $\pi_{RhRh}{}^*$ orbital upward through an n–$\pi_{RhRh}{}^*$ electronic interaction, which has pseudo-π symmetry with respect to the Rh–O axis. Carboxylate ligands have two such lone pairs, whereas amidate and amidinate ligands have one and none of such lone pairs, respectively. In this model, we expect that the substitution of the bridging ligand from a carboxylate to an amidate or to an amidinate would stabilize the $\pi_{RhRh}{}^*$ level, while the energy level of the $\delta_{RhRh}{}^*$ orbital remains less affected.

The second model is illustrated in Scheme II. The highest occupied π orbital on the bridging ligand (π_{br}) destabilizes the $\delta_{RhRh}{}^*$ orbital through a π-donative interaction from the ligands to the Rh_2 core. The destabilization is due to a Rh–bridging ligand π-antibonding character in the $\delta_{RhRh}{}^*$ orbital. This destabilization would be enhanced when the bridging ligand is an amidate or an amidinate in comparison to a carboxylate ligand, since the π_{br} levels in the formers are higher lying than that in the latter.

Scheme II will be shown in the next section to be consistent with the experimental results.

Ligand Dependence of Oxidation Potential and of Symmetry of Odd-Electron Orbital. Figure 4 summarizes electrochemical oxidation potentials of Rh_2^{4+} complexes together with the symmetries of the odd-electron orbitals of the corresponding Rh_2^{5+} radicals. The assignments of the odd-electron orbitals are based on our previous[8b,13] and present studies.

$[Rh_2(O_2CCH_3)_4L_2]^{\bullet+}$, where L is H_2O, CH_3OH, THF, $(CH_3)_2CO$, CH_3CN, and Cl^-, has an odd electron in the $\pi_{RhRh}{}^*$ orbital. Their parent Rh_2^{4+} complexes have most positive oxidation potentials in Figure 4. The oxidation potentials of those Rh_2^{4+} complexes, from which derived Rh_2^{5+} radicals have the $\delta_{RhRh}{}^*$ odd-electron orbitals, are less positive. These results indicate that the substitution of bridging ligands shifts not the energy level of the $\pi_{RhRh}{}^*$ orbital but the $\delta_{RhRh}{}^*$ level. The negative shift of the oxidation potential induced by the substitution of the NH or NR group for the oxygen atom in the bridging moiety[9,27,29,31-34] is a result of the destabilization of the $\delta_{RhRh}{}^*$ orbital. This is in accord with the Rh_2–bridging ligand interaction shown in Scheme II. Scheme I is not consistent with the present observations.

The present conclusion supports the analysis of the electronic configuration of Ru_2^{4+} complexes based on the Ru–Ru bond lengths and the spin multiplicities of $Ru_2(O_2CR)_4L_2$ and $Ru_2[(tol)NNN(tol)]_4$ reported by Cotton and Matusz,[35] where tol designates a *p*-methylphenyl group. The former complexes have a triplet ground state with a ($\sigma + \pi$) double-bond configuration of $\sigma^2\pi^4\delta^2\pi^{*2}\delta^{*2}$ [or less preferably a ($\sigma + 0.5\pi + 0.5\delta$) double-bond configuration of $\sigma^2\pi^4\delta^2\pi^{*3}\delta^{*1}$]. The latter complex has a diamagnetic ground state with a ($\sigma + \delta$) double-bond configuration of $\sigma^2\pi^4\delta^2\pi^{*4}$, resulting in a longer Ru–Ru bond length than those in the former complexes. This has been attributed to the enhanced upward shift of the $\delta_{RuRu}{}^*$ energy level relative to the $\pi_{RuRu}{}^*$ level induced by the azenidate bridging ligand.

The Rh_2^{5+} radicals with axial ligands of phosphines and phosphites have an odd electron in the σ_{RhRh} orbital.[8,9] Their parent Rh_2^{4+} complexes also have a large dependence of oxidation potentials on the bridging ligands (Figure 4). The substitution of an amidate ligand for a carboxylate bridge results in a negative shift of the potential, although the extent of the shift is about half that for complexes resulting in $\delta_{RhRh}{}^*$ radicals. We propose that this shift is induced by an increased mixing of the bridging-ligand orbitals into the σ_{RhRh} orbital in a Rh–bridging ligand σ-antibonding phase.

Acknowledgment. This work was supported by Grant-in-Aid for scientific research from the Ministry of Education, Science and Culture. We are grateful to Dr. Z. Ogumi (Kyoto University) for valuable discussions.

---

[30] Sowa, T.; Kawamura, T.; Shida, T.; Yonezawa, T. *Inorg. Chem.* **1983**, *22*, 56.

[31] Duncan, J.; Malinski, T.; Zhu, T. P.; Hu, Z. S.; Kadish, K. M.; Bear, J. L. *J. Am. Chem. Soc.* **1982**, *104*, 5507.

[32] Bear, J. L.; Zhu, T. P.; Malinski, T.; Dennis, A. M.; Kadish, K. M. *Inorg. Chem.* **1984**, *23*, 674.

[33] Zhu, T. P.; Ahsan, M. Q.; Malinski, T.; Dennis, A. M.; Kadish, K. M.; Bear, J. L. *Inorg. Chem.* **1984**, *23*, 2.

[34] Piraino, P.; Bruno, G.; Tresoldi, G.; Schiavo, S. L.; Zanello, P. *Inorg. Chem.* **1987**, *26*, 91.

[35] Cotton, F. A.; Matusz, M. *J. Am. Chem. Soc.* **1988**, *110*, 5761.